
Gradient Attention Map Based Verification of Deep Convolutional Neural Networks with Application to X-ray Image Datasets

Omid Halimi Milani¹, Amanda Nikho², Lauren Mills², Marouane Tliba³,
Ahmet Enis Cetin¹, Mohammed H. Elnagar²

¹Department of Electrical and Computer Engineering, University of Illinois Chicago, IL, USA

²Department of Orthodontics, College of Dentistry, University of Illinois Chicago, IL, USA

³University of Orleans, Orleans, France

Abstract

Deep learning models have great potential in medical imaging, including orthodontics and skeletal maturity assessment. However, applying a model to data different from its training set can lead to unreliable predictions that may impact patient care. To address this, we propose a comprehensive verification framework that evaluates model suitability through multiple complementary strategies. First, we introduce a Gradient Attention Map (GAM)-based approach that analyzes attention patterns using Grad-CAM and compares them via similarity metrics such as IoU, Dice Similarity, SSIM, Cosine Similarity, Pearson Correlation, KL Divergence, and Wasserstein Distance. Second, we extend verification to early convolutional feature maps, capturing structural misalignments missed by attention alone. Finally, we incorporate an additional garbage class into the classification model to explicitly reject out-of-distribution inputs. Experimental results demonstrate that these combined methods effectively identify unsuitable models and inputs, promoting safer and more reliable deployment of deep learning in medical imaging.

Keywords

Attention Misalignment, Medical Imaging, Model Suitability, Explainable AI, Deep Learning Verification

1 Introduction

Deep learning has significantly improved automated diagnostic capabilities in medical imaging, particularly in orthodontics and maxillofacial surgery, where precise classification of conditions is essential for treatment planning. Orthodontic diagnosis tasks require high model accuracy. Ensuring model suitability for specific datasets remains a challenge.

(i) If a model trained on one dataset is mistakenly tested on a completely different dataset, its decisions become unreliable. (ii) Transfer learning is widely used in practice. However,

minor training after transfer learning may not be enough to adapt the model effectively to new datasets. (iii) An unrelated image may be applied to the neural network by mistake, and the model will generate a result based solely on its training data, leading to incorrect classifications. Additionally, X-ray scanners may capture only a portion of an image or scan a corrupted image, causing the model to produce misleading results without recognizing the input as incomplete or corrupted.

Current evaluation methods primarily focus on performance metrics such as accuracy and confidence scores, which fail to indicate whether the model is inherently suitable for the test data.

In orthodontics, precise classification is crucial for determining the appropriate treatment pathway. For example, in Class III malocclusion diagnosis, lateral cephalometric X-rays and profile photographs are commonly used to classify whether a patient requires surgical intervention [6, 7]. Similarly, skeletal maturation assessment using cranial base synchondroses, such as the speno-occipital synchondrosis (SOS), is vital for forensic age estimation and orthodontic treatment planning [1, 2]. In both applications, misclassification can lead to incorrect diagnoses and suboptimal treatment decisions, emphasizing the need for reliable models.

Despite advancements in deep learning, model misapplication remains a critical issue. If a model trained on malocclusion classification is mistakenly tested on SOS data, it would likely generate incorrect predictions due to the fundamental differences in anatomical structures and classification objectives. Traditional evaluation methods, such as accuracy, precision, and recall, do not provide insight into whether the model was trained on a compatible dataset.

This problem necessitates a new model verification approach to ensure that a model is being used correctly. The key contributions of this work are as follows:

- Introduce a Gradient Attention Map-based approach to verify whether a deep learning model is suitable for a given dataset or an image.
- Develop a feature map-based verification method that analyzes early convolutional activations to capture structural inconsistencies beyond attention patterns.
- Introduce a garbage class strategy to explicitly detect out-of-distribution or misapplied inputs, improving both model robustness and classification performance.
- Enhance model explainability by systematically evaluating model attention and feature patterns to ensure reliability in clinical deployment.

2 X-ray Image Datasets

Deep learning models for medical imaging require datasets that are well-annotated and clinically validated to ensure reliability. This study utilizes two distinct datasets: one for speno-occipital synchondrosis (SOS) fusion staging and another for Class III malocclusion classification using lateral cephalometric X-rays. Both datasets are carefully curated to support automated classification tasks while addressing the challenge of model verification.

2.1 SOS Fusion Staging Dataset

This dataset consists of cone-beam computed tomography (CBCT) scans collected from patients with varying stages of spheno-occipital synchondrosis fusion.

To standardize the dataset, each CBCT scan was preprocessed. The region of interest (ROI) was extracted through manual segmentation by expert, aligning the planes to ensure consistency.

2.2 Class III Malocclusion X-ray Dataset

This dataset consists of lateral cephalometric X-ray images: orthodontic camouflage and surgical intervention.

Each patient record includes X-ray images paired with expert annotations.

The dataset was curated to include only cases with confirmed successful treatment outcomes, ensuring that the classification labels reflect reliable clinical decisions.

3 Methodology

After curating and preprocessing the dataset for consistency and reliability, we utilize advanced deep learning models for automated classification. Pre-trained models known for their robustness in image analysis are employed to enhance classification accuracy while reducing the need for extensive new model training. The selected models include ResNet18, ResNet34, ResNet50, ConvNeXt, and ConvNeXt with attention mechanisms. These models have been fully trained and have demonstrated strong performance in classification tasks [3, 4, 21, 21].

3.1 Model Verification Using Grad-CAM Similarity Metrics

To quantify the alignment of candidate models with the reference model, we compute statistical similarity metrics between their Grad-CAM attention maps. These metrics capture spatial, structural, and distributional differences, enabling a robust evaluation of attention alignment [5, 8, 11].

3.1.1 Grad-CAM Computation

For each input image I , the Grad-CAM heatmap $H_M(I)$ for a given model M is computed as:

$$H_M(I) = \text{ReLU} \left(\sum_k \alpha_k A_k \right) \quad (1)$$

3.1.2 Threshold-Based Binarization

To obtain a fair comparison, we convert raw Grad-CAM heatmaps into binary masks using a median thresholding approach [9]:

$$B_M(i, j) = \begin{cases} 1, & H_M(i, j) > \text{median}(H_M) \\ 0, & \text{otherwise} \end{cases} \quad (2)$$

where $B_M(i, j)$ represents the binarized attention region for model M .

3.1.3 Spatial Overlap Metrics

To measure the degree of similarity between the reference and candidate model’s focus regions, we compute the Intersection over Union (IoU) and Dice Similarity Coefficient (DSC) [10–12]:

$$\text{IoU}(M_1, M_2) = \frac{|B_{M_1} \cap B_{M_2}|}{|B_{M_1} \cup B_{M_2}|} \quad (3)$$

$$\text{DSC}(M_1, M_2) = \frac{2|B_{M_1} \cap B_{M_2}|}{|B_{M_1}| + |B_{M_2}|} \quad (4)$$

3.1.4 Perceptual Similarity Assessment

To further analyze attention alignment, we compute the Structural Similarity Index (SSIM), which captures perceptual differences in intensity distribution:

$$\text{SSIM}(M_1, M_2) = \frac{(2\mu_{M_1}\mu_{M_2} + C_1)(2\sigma_{M_1M_2} + C_2)}{(\mu_{M_1}^2 + \mu_{M_2}^2 + C_1)(\sigma_{M_1}^2 + \sigma_{M_2}^2 + C_2)} \quad (5)$$

[13–15].

3.1.5 Statistical Correlation Analysis

To measure linear alignment in pixel intensities, we compute Cosine Similarity and Pearson Correlation [16, 17]:

$$\text{Cosine}(M_1, M_2) = \frac{H_{M_1} \cdot H_{M_2}}{\|H_{M_1}\| \|H_{M_2}\|} \quad (6)$$

$$r(M_1, M_2) = \frac{\sum(H_{M_1} - \bar{H}_{M_1})(H_{M_2} - \bar{H}_{M_2})}{\sqrt{\sum(H_{M_1} - \bar{H}_{M_1})^2} \sqrt{\sum(H_{M_2} - \bar{H}_{M_2})^2}} \quad (7)$$

3.1.6 Distributional Divergence Measures

To assess differences in the probability distributions of attention maps, we compute Kullback-Leibler (KL) Divergence and Wasserstein Distance [18–20]:

$$D_{KL}(P_{M_1} \| P_{M_2}) = \sum_i P_{M_1}(i) \log \frac{P_{M_1}(i)}{P_{M_2}(i) + \epsilon} \quad (8)$$

$$W(P_{M_1}, P_{M_2}) = \sum_i d(i) |P_{M_1}(i) - P_{M_2}(i)| \quad (9)$$

3.1.7 Integrating Similarity Metrics into the Verification Framework

The computed similarity metrics serve as features for a Random Forest classifier, enabling automated differentiation between well-aligned and misaligned models. By learning from these statistical patterns, the framework systematically identifies models whose attention maps exhibit clinically meaningful alignment with expert-defined regions, ensuring more reliable deep learning-based decision-making.

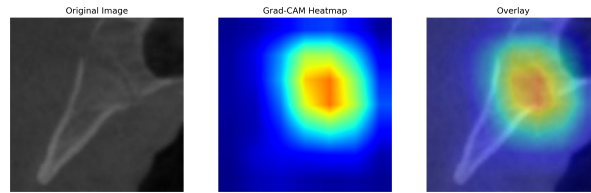


Figure 1: Grad-CAM visualization for a model trained and tested on the SOS dataset. The attention is well-aligned with the anatomical structures, highlighting relevant areas.

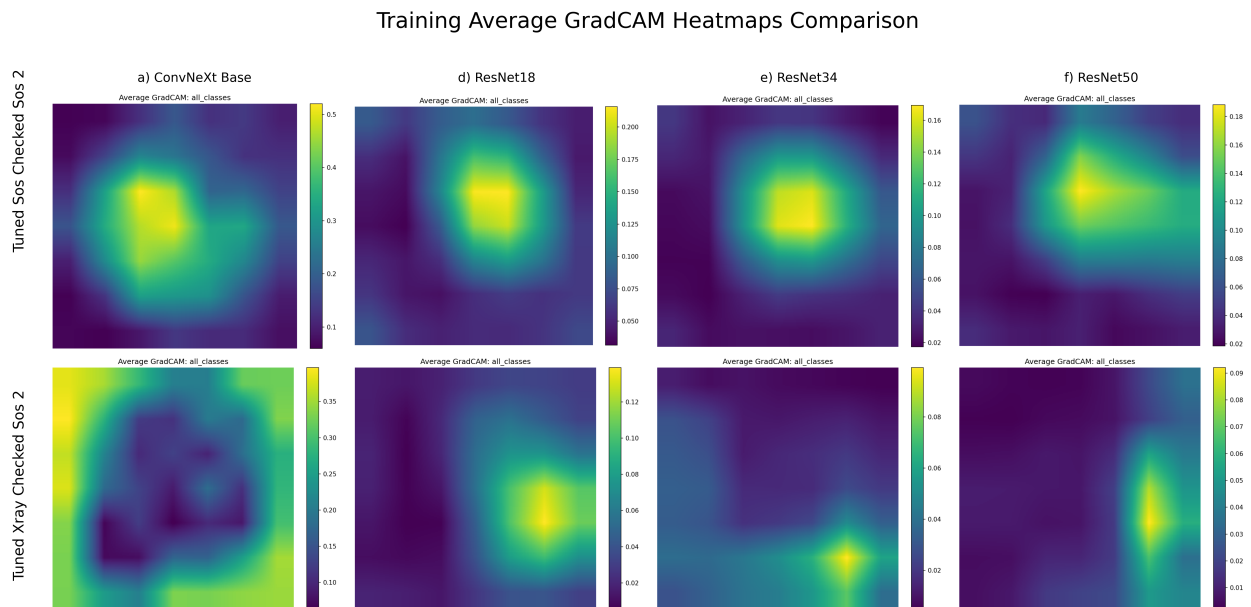


Figure 2: Visualization of the average Gradient Attention Maps (GAMs) for each model during training. The first row represents attention maps for models trained on the SOS dataset and evaluated on the SOS training set. The second row shows attention maps for models trained on the Class III dataset and tested on the SOS training set. The heatmaps illustrate where each model focuses when making predictions.

3.2 Random Forest-based Model Verification and Rejection Strategy

Traditional evaluation metrics, such as classification accuracy, fail to indicate whether a neural network model is genuinely suitable for a specific classification task. A model may achieve high accuracy during training while relying on spurious correlations or focusing on irrelevant anatomical features, leading to unreliable decision-making in real-world clinical applications. To address this challenge, we introduce a random forest-based model verification framework using interpretable learning-based classification.

Our approach trains a classification model to distinguish between clinically meaningful and misaligned attention patterns. The Random Forest classifier learns patterns in attention alignment by leveraging statistical representations of Grad-CAM differences, distinguishing valid models from those with inconsistent or irrelevant focus regions using the features described in the previous section.

This method improves model selection by quantifying how well a model mimics expert decision-making, contributing to a more transparent and explainable AI-driven clinical workflow. By systematically rejecting models with misaligned focus regions, we ensure that only models that correctly align their attention with expert-defined regions are considered suitable.

The effectiveness of this approach is demonstrated in Fig. 1, which shows a Grad-CAM visualization for a model trained and tested on the SOS dataset. The model correctly attends to relevant anatomical structures, highlighting the importance of attention alignment as an evaluation metric beyond traditional performance scores.

3.3 Feature Map-Based Verification via Internal Representations (Method 2)

To further enhance model verification, we extract internal feature maps from early convolutional layers of the network. These feature maps often contain edge-like or low-level patterns that can indicate whether the model is processing the input in a clinically meaningful manner.

Let $f_i(k, l)$ denote the activation value at location (k, l) from the i -th filter of a selected convolutional layer. We define the overall feature response at location (k, l) as:

$$S(k, l) = \sum_i |f_i(k, l)| \quad (10)$$

Since ReLU activation ensures non-negativity, $S(k, l)$ can be treated as a 2D distribution. We compute these maps for both the candidate and reference models across Layer 1 and Layer 2. Then, the same suite of similarity metrics (IoU, Dice, SSIM, Cosine, Pearson, KL, and Wasserstein) is used to compare these distributions.

This method is particularly effective in detecting models trained on unrelated datasets or misaligned input data. Random forest classifiers trained on these similarity features can distinguish between suitable and unsuitable models, even when classification accuracy appears acceptable.

Table 1: Performance Comparison of Selected Models on CLASS III (Chin) and SOS Datasets

Model	CLASS III - Chin				SOS Dataset			
	Accuracy	Precision	Recall	F1-Score	Accuracy	Precision	Recall	F1-Score
ResNet-18	86.36	88.60	90.18	89.38	72.55	72.12	72.55	70.84
ResNet-34	87.50	88.79	91.96	90.35	75.07	75.01	75.07	74.05
ResNet-50	85.80	92.23	84.82	88.37	74.79	74.08	74.79	73.79
ConvNeXt	90.91	92.11	93.75	92.92	78.99	78.57	78.99	78.35
ConvNeXt+Attn (reference model)	-	-	-	-	79.97	80.65	79.97	78.87

3.4 Garbage Class Strategy for Rejecting Out-of-Distribution Inputs (Method 3)

We also introduce an auxiliary strategy based on extending the classification space. Instead of designing binary or multi-class classifiers alone, we define a new $k + 1$ -class classification problem where the additional class represents "non-target" or out-of-distribution samples.

For instance, in the case of 5-stage SOS classification, we define a 6-class network where the sixth class corresponds to inputs that do not belong to any SOS category (e.g., Chin or CVM images). This garbage class is trained using irrelevant but structurally similar X-ray images.

During inference, the model can effectively reject unfamiliar inputs by assigning them to the $k + 1$ -th class. This technique acts as a built-in verification mechanism and prevents the network from forcing a prediction on unsuitable data.

Our experiments show that models with this extended class formulation achieve better robustness and produce highly accurate classifications for suitable inputs, while flagging mismatched ones for rejection.

4 Results and Evaluation

To demonstrate our verification framework, we visualize average Gradient Attention Maps (GAMs) from models trained and tested on the SOS dataset versus those trained on Class III data and tested on SOS. As shown in Figure 2, SOS-trained models focus on relevant anatomical regions, while Class III-trained models exhibit misaligned attention.

Table 1 presents the performance comparison of selected deep learning models on two datasets: CLASS III (X-ray) and the SOS dataset. The evaluation metrics include Accuracy, Precision, Recall, and F1-Score. The results indicate that ConvNeXt outperforms other models in both datasets, achieving the highest scores across all metrics in CLASS III and showing competitive performance on the SOS dataset. The reference model, ConvNeXt+Attn, is only evaluated on the SOS dataset, where it achieves the best overall performance, surpassing all other models. These results highlight the effectiveness of attention-based architectures in improving model generalization and robustness across different datasets.

The effectiveness of our verification approach is further reinforced by Figure 2, which consolidates the GAM comparisons across models. This demonstrates how our method systematically removes models that focus on incorrect features while retaining those with aligned attention patterns, ensuring that models are not only performing well in terms of

Table 2: Performance of the Random Forest Model

Model	Accuracy (%)	Precision (%)	Recall (%)	F1-Score (%)	ROC AUC (%)
Random Forest	87.54	87.54	87.54	87.55	93.52

accuracy but also making clinically meaningful decisions.

4.1 Model Verification Outcomes

The proposed model verification framework effectively identifies models that align with the expected learning patterns by leveraging interpretable decision models trained on features extracted from Gradient Attention Maps (GAMs). This approach ensures that only models optimized for the SOS dataset are retained, preventing the inclusion of models trained on unrelated data that could compromise clinical decision-making.

Instead of relying on predefined separation values, we employ a random forest classifier trained to recognize patterns in how models attend to different anatomical regions. By extracting statistical representations of GAM differences between a reference model and candidate models, the classifier learns distinguishing characteristics that differentiate well-aligned models from those that focus on irrelevant or inconsistent regions.

Our evaluation demonstrates that this method successfully filters out models that do not exhibit alignment with clinically meaningful features. Even among models trained on the SOS dataset, those showing inconsistent GAM patterns—indicating attention to incorrect anatomical structures—were effectively excluded. This underscores the importance of attention-based model validation, ensuring that deep learning models focus on relevant medical regions rather than just maximizing traditional performance metrics.

For evaluation, we compute the gradient attention map for each sample and compare it against the reference average gradient attention map. From this comparison, we extract seven similarity features that quantify spatial, perceptual, and statistical similarities between the attention maps. This results in a dataset of 586 data points, where each sample is characterized by these seven features.

Among these data points, 312 are classified as *not acceptable*, meaning they were tested on a model that was not trained on similar data, while 274 are categorized as *acceptable*, indicating they were tested on a model trained on similar data.

To assess the model’s performance, we apply 5-fold cross-validation using a random forest classifier. The model achieves a Receiver Operating Characteristic - Area Under the Curve (ROC AUC) score of 93.52%, with an overall accuracy of 87.54%. The precision, recall, and F1-score are consistently around 87.54%, with an average F1-score of 87.55% across all samples.

By leveraging an interpretable learning-based approach, we ensure that models exhibiting attention inconsistencies are systematically identified and removed.

Table 3: Validation Statistics of Grad-CAM Similarity Metrics for Misaligned (Label 0) and Aligned (Label 1) Models

Metric	Label	Mean	Min	Max	Std
IoU	0	0.3168	0.0000	0.7930	0.1824
Dice	0	0.4516	0.0000	0.8845	0.2181
SSIM	0	0.1980	0.0233	0.7011	0.1167
Cosine	0	0.3887	0.0261	0.8755	0.2219
Pearson	0	-0.0193	-0.7909	0.8063	0.4029
KL Divergence	0	7.1166	0.2194	17.7622	4.7189
Wasserstein	0	0.1714	0.0681	0.2792	0.0350
IoU	1	0.4558	0.0828	0.7770	0.1492
Dice	1	0.6116	0.1529	0.8745	0.1443
SSIM	1	0.3845	0.0902	0.7038	0.1309
Cosine	1	0.6952	0.1561	0.9559	0.1749
Pearson	1	0.4037	-0.7668	0.9403	0.3782
KL Divergence	1	3.2797	0.1644	12.2506	2.4379
Wasserstein	1	0.1297	0.0602	0.2010	0.0358

4.2 Feature Map-Based Verification Results (Method 2)

We further evaluate the model’s suitability using internal representations extracted from the first and second convolutional layers. These feature maps are transformed into probability distributions and compared using the same seven similarity metrics as in Method 1. A Random Forest classifier is trained to distinguish between suitable and unsuitable models.

Table 4 shows that using Layer 1 activations from a model trained on the Chin dataset and tested on SOS samples results in near-perfect performance, with 99.36% accuracy and 99.96% ROC AUC. The performance slightly drops when testing against rotated SOS images, yet it remains robust above 79%.

Table 4: Rotation Robustness Comparison using Feature Map-Based Verification (Method 2)

Model	Train	Test	Accuracy	ROC AUC	F1 (avg)
Layer 1	Chin	SOS	0.9936	0.9996	0.9936
Gradient-Based	Chin	SOS	0.8754	0.9358	0.8749
Layer 1	SOS	Rotated SOS	0.8013	0.8825	0.8005
Layer 2	SOS	Rotated SOS	0.7917	0.8690	0.7912

4.3 Garbage Class Strategy Results (Method 3)

To detect out-of-distribution inputs, we introduce a $k + 1$ class for models originally trained for k -class classification. This additional "garbage" class is trained using unrelated datasets such as Chin or CVM samples.

Tables 5 and 6 demonstrate that the 6th class achieves perfect 1.00 precision, recall, and F1-score, indicating its ability to correctly isolate mismatched data. Moreover, overall model accuracy increases when using this approach, showing not only its rejection power but also enhanced performance.

With Chin as the 6th class:

Table 5: Classification with Chin as Garbage Class (Method 3)

Class	Precision	Recall	F1-Score	Support
1	0.92	0.92	0.92	159
2	0.78	0.73	0.75	92
3	0.71	0.82	0.76	92
4	0.70	0.62	0.66	125
5	0.88	0.89	0.89	255
6	1.00	1.00	1.00	176
Avg	0.83	0.83	0.83	899

With CVM as the 6th class:

Table 6: Classification with CVM as Garbage Class (Method 3)

Class	Precision	Recall	F1-Score	Support
1	0.86	0.91	0.88	159
2	0.69	0.68	0.69	92
3	0.72	0.74	0.73	92
4	0.70	0.57	0.63	125
5	0.87	0.91	0.89	255
6	1.00	1.00	1.00	181
Avg	0.81	0.80	0.80	904

5 Conclusion

We proposed a verification framework that assesses the suitability of deep learning models in medical imaging by analyzing Gradient Attention Maps (GAM). Beyond Grad-CAM-based verification, we introduced a feature map-based method using early convolutional activations, and a garbage class strategy to reject out-of-distribution inputs. Together, these approaches

enhance model reliability and prevent misapplication. Future work will focus on extending the framework to multi-modal datasets.

Acknowledgment

This material is based upon work supported by the National Science Foundation under Award No. 2303700.

References

- [1] Powell, T. V., and Brodie, A. G. (1963). Closure of the spheno-occipital synchondrosis. *The Anatomical Record*, 147(1), 15–23.
- [2] Al-Gumaei, W. S., Al-Attab, R., Al-Tayar, B., et al. (2022). Comparison of spheno-occipital synchondrosis maturation stages with three-dimensional assessment of mandibular growth. *BMC Oral Health*, 22(1), 654.
- [3] He, K., Zhang, X., Ren, S., and Sun, J. (2016). Deep residual learning for image recognition. In *Proceedings of the IEEE Conference on Computer Vision and Pattern Recognition*, 770–778.
- [4] Liu, Z., Mao, H., Wu, C.-Y., Feichtenhofer, C., Darrell, T., and Xie, S. (2022). A convnet for the 2020s. In *Proceedings of the IEEE/CVF Conference on Computer Vision and Pattern Recognition (CVPR)*, 11976–11986. IEEE.
- [5] Selvaraju, R. R., Cogswell, M., Das, A., Vedantam, R., Parikh, D., and Batra, D. (2017). Grad-CAM: Visual explanations from deep networks via gradient-based localization. In *Proceedings of the IEEE International Conference on Computer Vision*, 618–626.
- [6] Lisboa, C. de O., et al. (2017). Orthodontic-surgical retreatment of facial asymmetry with occlusal cant and severe root resorption: A 3-year follow-up. *American Journal of Orthodontics and Dentofacial Orthopedics*, 152(2), 268–280.
- [7] Kawai, N., et al. (2021). Treatment decision of camouflage or surgical orthodontic treatment for skeletal Class III patients based on analysis of masticatory function. *Journal of Dental Sciences*, S1991790221002464.
- [8] LeCun, Y., Bottou, L., Bengio, Y., and Haffner, P. (1998). Gradient-based learning applied to document recognition. *Proceedings of the IEEE*, 86(11), 2278–2324.
- [9] Doshi-Velez, F., and Kim, B. (2017). Towards a rigorous science of interpretable machine learning. *arXiv preprint arXiv:1702.08608*.
- [10] Pellano, K. N., Strümke, I., and Ihlen, E. A. F. (2024). From movements to metrics: Evaluating explainable AI methods in skeleton-based human activity recognition. *Sensors*, 24(6), 1940.

-
- [11] Livieris, I. E., Pintelas, E., Kiriakidou, N., and Pintelas, P. (2023). Explainable image similarity: Integrating Siamese networks and Grad-CAM. *Journal of Imaging*, 9(10), 224.
- [12] Adebayo, J., Gilmer, J., Muelly, M., Goodfellow, I., Hardt, M., and Kim, B. (2018). Sanity checks for saliency maps. *Advances in Neural Information Processing Systems*, 31.
- [13] Hase, P., and Bansal, M. (2020). Evaluating explainable AI: Which algorithmic explanations help users predict model behavior? *arXiv preprint arXiv:2005.01831*.
- [14] Selvaraju, R. R., Cogswell, M., Das, A., Vedantam, R., Parikh, D., and Batra, D. (2020). Grad-CAM: Visual explanations from deep networks via gradient-based localization. *International Journal of Computer Vision*, 128, 336–359.
- [15] Samek, W., Montavon, G., Vedaldi, A., Hansen, L. K., and Müller, K.-R. (2019). *Explainable AI: Interpreting, explaining and visualizing deep learning* (Vol. 11700). Springer Nature.
- [16] Ras, G., Xie, N., Van Gerven, M., and Doran, D. (2022). Explainable deep learning: A field guide for the uninitiated. *Journal of Artificial Intelligence Research*, 73, 329–396.
- [17] Li, X.-H., Shi, Y., Li, H., Bai, W., Cao, C. C., and Chen, L. (2021). An experimental study of quantitative evaluations on saliency methods. In *Proceedings of the 27th ACM SIGKDD Conference on Knowledge Discovery & Data Mining*, 3200–3208.
- [18] Chakraborty, T., Trehan, U., Mallat, K., and Dugelay, J.-L. (2022). Generalizing adversarial explanations with Grad-CAM. In *Proceedings of the IEEE/CVF Conference on Computer Vision and Pattern Recognition*, 187–193.
- [19] Chaddad, A., Peng, J., Xu, J., and Bouridane, A. (2023). Survey of explainable AI techniques in healthcare. *Sensors*, 23(2), 634.
- [20] Panaretos, V. M., and Zemel, Y. (2019). Statistical aspects of Wasserstein distances. *Annual Review of Statistics and Its Application*, 6(1), 405–431.
- [21] Koonce, B. (2021). ResNet 34. In *Convolutional Neural Networks with Swift for TensorFlow: Image Recognition and Dataset Categorization*, 51–61. Springer.